

MIXING DRIVEN BY INTERNAL KELVIN WAVES IN LARGE LAKES AND THE COASTAL OCEANS

G.N. IVEY¹ and T. MAXWORTHY²

¹Centre for Water Research, University of Western Australia, Nedlands, WA 6009, AUSTRALIA

²Dept Mechanical & Aerospace Engineering, University of Southern California, Los Angeles CA, USA

ABSTRACT

We describe a laboratory study of one mechanism for driving horizontal exchange or mixing in the coastal regions of lakes or seas. In response to an applied wind stress on the surface of a density stratified lakes or sea, internal Kelvin waves form and propagate around the shoreline with a strong velocity signature in the near-shore region. The laboratory experiments demonstrate that this flow can interact with the shoreline topography to form large scale two dimensional eddies, which subsequently controls the horizontal mixing between the nearshore and offshore regions.

INTRODUCTION

When a wind stress is applied to the surface of a large stratified lake or sea, the initial fluid response consists of a setup of the free surface against the coastline in the downwind direction and a corresponding setdown of the interface separating fluid layers of different density. The system then adjusts and, in the case of large water bodies where rotation is important, internal Kelvin waves form and propagate along the shore away from the region of setdown. In smaller water bodies, where rotation is unimportant, the internal seiche is the analogous large scale internal wave response. Internal Kelvin waves created by wind events, or by variations in riverine inflow rates, have been observed in a number of water bodies (e.g. Lake Geneva (Mortimer, 1963, 1974), Lake Ontario (Csanady and Scott 1974), Kamloops Lake (Hamblin 1978), the Bodensee (Zenger 1989)). In large water bodies the effect of the wind stress is thus particularly effective in creating large scale internal waves and strong flows in the near-shore regions. Field observations (e.g. Zenger 1989) also show that these waves are rapidly dissipated in just a few cycles, indicating that large amounts of energy have been lost in the near-shore region. Natural water bodies such as the Bodensee or Lake Biwa in Japan typically possess complex shorelines with large bays and side inlets around the periphery of the main basin. For environmental reasons there is considerable interest in understanding the flushing and exchange mechanisms between these inlets and the main basin (e.g. Okamoto 1991). The present experiments were designed to investigate the mechanism whereby these Kelvin waves are dissipated and the implications for mixing between the nearshore and the offshore regions.

INTERNAL WAVE GENERATION

In response to an applied wind stress on the surface of a two layer stratified water body, a series of baroclinic Kelvin waves propagate along the boundaries (Csanady and Scott (1974)). The waves have a displacement at the density interface of the form

$$\zeta = a \exp\left(-\frac{y}{R}\right) \cos(x - ct) \quad (1)$$

where a is the amplitude of displacement at the shore $y = 0$, x is the coordinate along the shore, the internal wave speed is $c = (g'h_1h_2/(h_1 + h_2))^{1/2}$ with $g' = (\rho_1 - \rho_2)/\rho_2$, where the subscripts refer to the upper and lower layers, respectively,

$R = c/f$ is the internal radius of deformation and f is the local Coriolis parameter.

Renouard (1981) examined the response to a suddenly applied constant wind stress in a laboratory study in a rectangular tank and noted the Kelvin waves decayed after several cycles, where a cycle is defined as the time of travel around the periphery of the basin. As Csanady and Scott (1974) pointed out, the duration of a typical storm is short compared to the time scale it takes for a wave to travel around the basin $T_n = P/c$, where P is the perimeter of the basin. Thus rather than the problem of steady forcing due to a step input, the more relevant problem from the point of view of application to lakes is the problem of time varying forcing.

LABORATORY EXPERIMENTS

The experiments were conducted in a rectangular perspex tank 2.0 m long, 0.6 m wide and 0.3 m deep and filled with a two-layer density stratified fluid. The entire tank was suspended on a pair of centrally-located bearings. To generate waves, the tank was then rocked up and down by use of a small DC motor located at one end underneath the tank and driving the tank via an eccentric crank and arm mechanism. This allowed the tank to be either tilted suddenly or to be rocked in a continuous sinusoidal fashion where both the frequency and amplitude of oscillation could be varied, and the entire assembly was mounted on a rotating turntable (see Figure 1). In the experiments the tilting of the tank was monitored by a displacement transducer mounted on the rotating table and measurements of the internal wave field induced by the rocking were made with three ultrasonic internal wave gauges. An L-shaped partition was installed at one end of the tank to form a relatively long narrow embayment - an arrangement suggested by the physical configuration of the Bodensee and Lake Biwa. The embayment width was varied during the runs and some tests were also conducted with the addition of bottom topography in the embayment. For the experiments described here, the tank was filled with a two-layer salt stratified fluid with layer depths typically in the ratio of 1:4 or 1:5, as suggested by the ratio of layer depths in the field observations. All densities were measured with a digital densimeter.

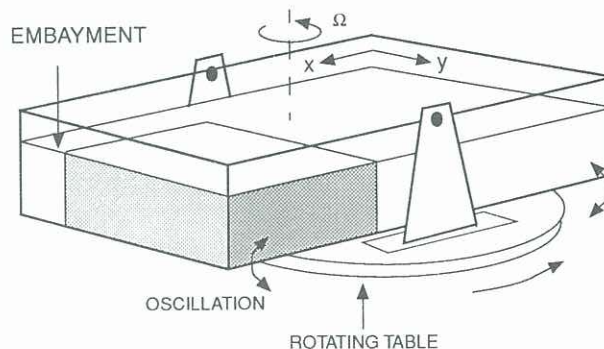


Figure 1. Schematic of experimental configuration showing coordinate definitions.

Consider first the case with no embayment and a simple rectangular geometry. Figure 2 shows a typical time series of the internal wave field created by suddenly tilting the tank. In response to this forcing we initially see a quite asymmetric wave profile about the equilibrium interface position with large excursions below the equilibrium position of order 1 cm close to the wall. Comparing Figures 2a, b and c we see the rapid decrease in wave amplitude with distance offshore at any instant in time, and all traces show an asymptotic approach of the interface to the final equilibrium position. Some 5 wave cycles are observed before the wave has decayed. Also note the appearance of small scale features on the wave crests, starting with the arrival of the second crest around $t = 120$ seconds, and continuing with each subsequent crest. Visual observation indicated small scale mixing was occurring in the tank which appeared to be initiated in the corner regions as the wave turned, consistent with the occurrence of the small scale instabilities on the crests. For the example shown in Figure 2, the internal wave speed was $c = 9.4 \text{ cms}^{-1}$ and thus the time of travel around the perimeter of the tank was 55.3 s, corresponding closely with the time interval between arrival of successive crests or troughs.

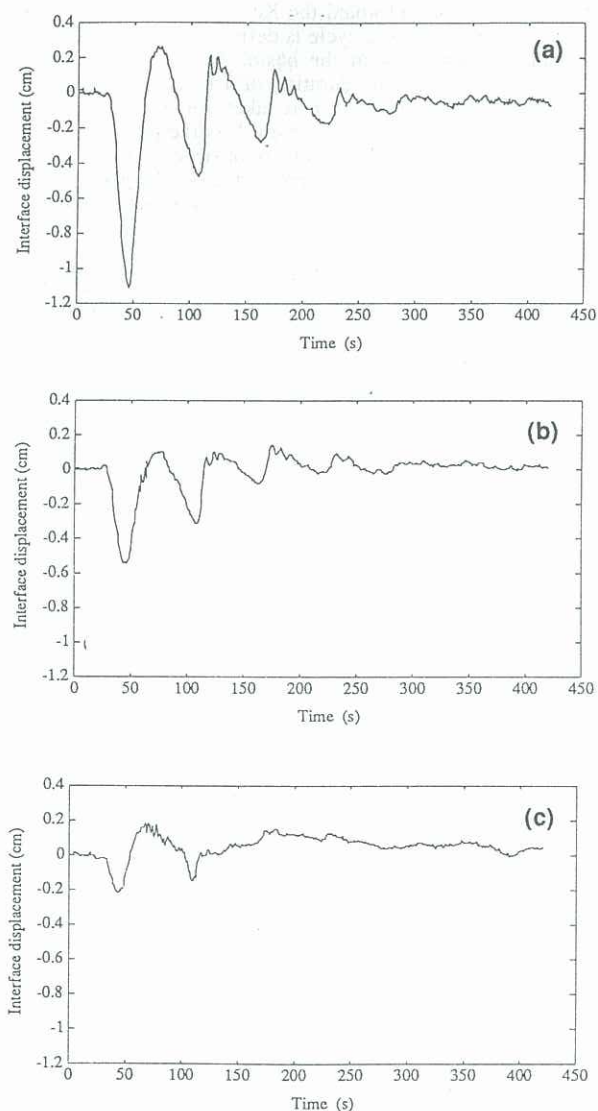


Figure 2. Internal wave response to step forcing in rectangular tank. Records were taken at $x = 100$ cm and $y = 1.7, 6.2$ and 13.0 cm in a, b and c, respectively, with $h_1 = 4$ cm, $h_2 = 14$ cm, $g' = 25.7 \text{ cms}^{-2}$, $f = 1.0 \text{ rs}^{-1}$, and deformation radius $R = 8.9$ cm.

The embayment was then fixed in position in the tank using the configuration shown in Figure 1. With the field observations in the Bodensee and Lake Biwa in mind, the width of the embayment was set at 15 cm which is slightly larger than the Rossby radius of deformation of order 8 to 10 cm used in these initial experiments. A transient test was conducted in exactly the same manner as before by rapidly tilting the tank to a new equilibrium position with typical results shown in Figure 3. Again there was a rapid decay of wave amplitude with distance offshore. In this case the internal wave speed was 8.9 cms^{-1} and the time of travel around the periphery of the main basin was 58.4 seconds, which compares closely with the arrival time of successive crests or troughs at the measurement site in Figure 3. In this sense the results shown in Figures 2 and 3 are similar in that they both indicate a Kelvin wave type response to the forcing. Comparing the two figures, it is clear that the embayment has resulted in a much more rapid dissipation of wave energy as the wave-induced flow was being modified by interaction with the complex topography.

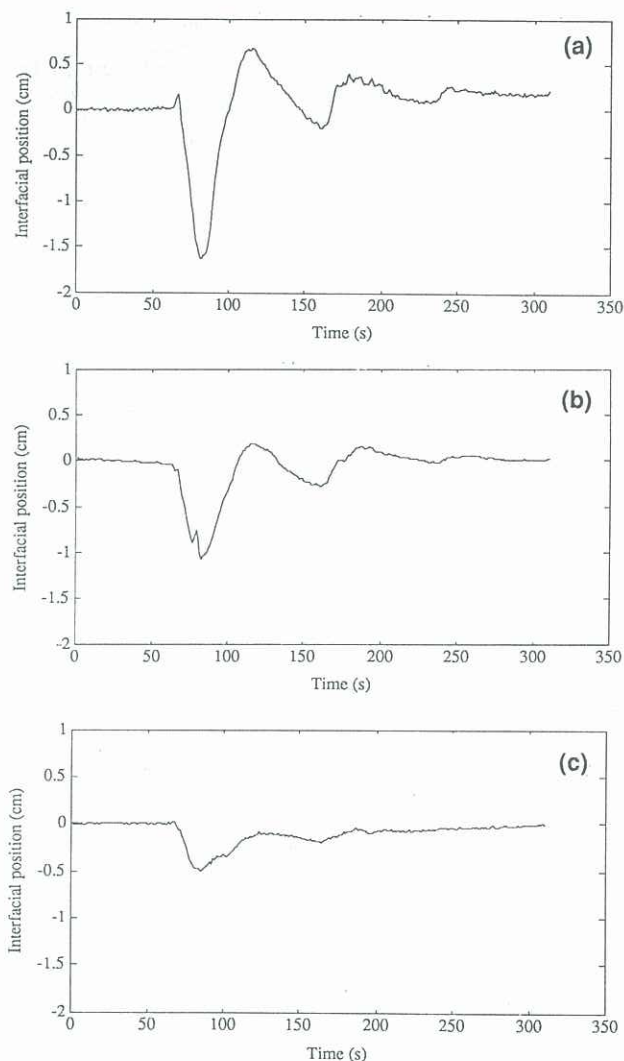


Figure 3. Internal wave response to step forcing in rectangular tank with embayment in position. Records were taken at $x = 80$ cm and $y = 1.0, 5.5$ and 12.5 cm in a, b and c, respectively, with $h_1 = 4$ cm, $h_2 = 14$ cm, $g' = 29.4 \text{ cms}^{-2}$ and $f = 1.0 \text{ rs}^{-1}$.

We were able to simulate the process of multiple wind events by continuously rocking the tank in a sinusoidal fashion with period T . As argued above, an important parameter in real lakes is the time scale of the forcing relative to the natural response time scale of the lake and figure 4 shows the result of varying forcing frequency. As can be

seen, changing the forcing timescale had a dramatic effect on the observed amplitude of the wave with a distinct peak in the mid-range near a period of $T = T_n$. For the case shown in Figure 4 the internal wave speed was 9.2 cms^{-1} and for the main basin in the tank (i.e. ignoring the embayment in Figure 1) the length of the basin P was 440 cm , hence the natural or travel time around the basin $T_n = 47.8 \text{ seconds}$ is independent of either forcing or rotation period. If the forcing period exactly coincided with T_n then there would be a reinforcement of the initial propagating wave - i.e. a resonance phenomena occurred. The forcing periods in Figure 4 are non-dimensionalised by T_n and indeed maximal response is observed in a fairly narrow band of forcing frequencies around the period $T = T_n$ with amplitudes greatly in excess of the forcing amplitude of 1 cm . As amplitudes were constrained even at the resonance period, damping effects were clearly important in the system and will be of two kinds: small scale viscous dissipation in the side-wall and bottom Ekman layers, and large scale losses associated with the interaction of the wave-induced flow and the topography as discussed below.

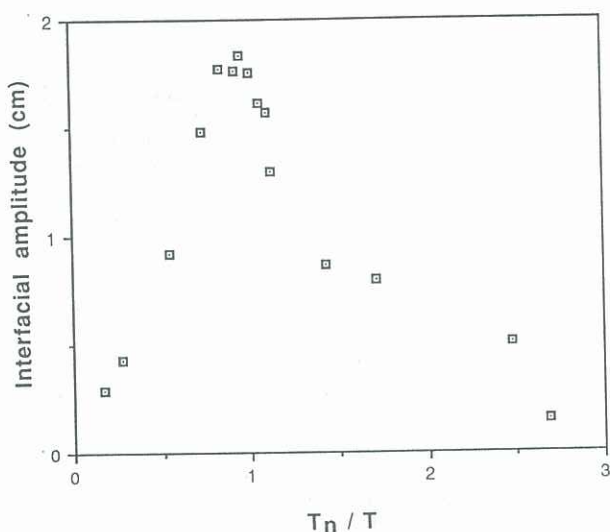


Figure 4: Internal wave amplitude as a function of forcing period. Records were taken at $x = 60 \text{ cm}$, $y = 0.5 \text{ cm}$ with $h_1 = 4.0 \text{ cm}$, $h_2 = 16 \text{ cm}$, $g' = 27.1 \text{ cms}^{-2}$ and $f = 0.58 \text{ rs}^{-1}$. Measured forcing periods T were non-dimensionalised by $T_n = 47.8 \text{ s}$.

The damping of the waves should also be influenced by the scale of the topographic features relative to the Rossby radius of deformation. Experiments were conducted by rocking the tank in a steady fashion, then measuring the time of decay of the internal wave field after the cessation of rocking. The damping timescale was taken as the time it takes for the wave amplitude to decay to 15% of the initial steady state value, or approximately $2 e$ -folding timescales if it were a simple exponential decay. The embayment width W was systematically varied relative to the Rossby radius of deformation R and the results shown in Figure 5 as a function of the Burger number S - the ratio of these two lengthscales. If the scale of the topography is small compared to the Rossby radius, then the decay of the Kelvin wave is little affected by the presence of the embayment and damping timescales are about 8 periods. Conversely, once the embayment width and Rossby radius are comparable, we see the damping is much more rapid with damping timescales of less than 4 periods for Burger numbers less than 1.

These observations of the wave field indicate an enhanced energy loss due to the presence of the embayment and the nature of the mixing associated with this loss is demonstrated by a simple dye injection study. The experimental tank was rocked in a steady harmonic fashion with the forcing amplitude chosen so as to give maximum

wave amplitude, and hence, induced fluid velocity. After running for many cycles, dye was steadily injected during a period of approximately 30 seconds from a single point in the lower layer on one side of the throat where the main basin joined the embayment.

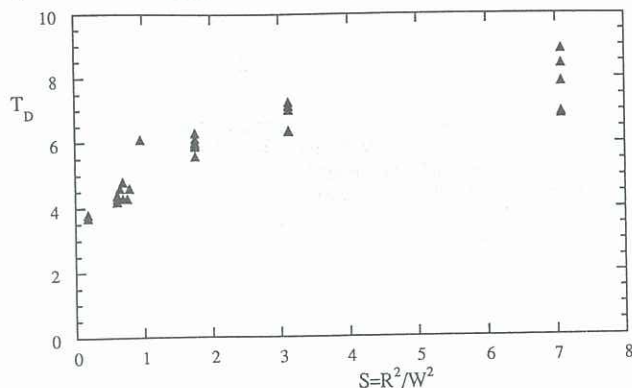


Figure 5. Damping timescale as a function of Burger number.

Initially, there was a strong ebb flow out of the bay in the lower layer (and a similar flood flow into the embayment in the upper layer associated with the strong baroclinic flows in each layer). This ebb flow separated from the sharp leading edge to form an eddy pair, with a well defined cyclone and a less well defined anticyclone, which propagated out into the main basin (Figure 6). As the flow reversed with the arrival of the next wave the eddy pair structure broke up. The cyclonic eddy retained its coherency and position, while the anticyclonic eddy was sheared out by the strong flood flow back into the embayment and the dye was swept back into the embayment. There was some tendency for separation as the flood flow entered the throat, although not as strongly as on the ebb phase. As the flow started to reverse, the production of a counter-rotating eddy pair and a strong ejection of fluid out of the embayment may be identified (Figure 6b). Over large time scales, the cyclonic eddies contributed to a cavity-scale cyclonic circulation in the main basin. The same dye studies revealed little evidence of vertical transfer of dye between the two layers in the embayment region, indicating small scale vertical mixing was negligible in comparison with the strong horizontal stirring or mixing driven by the large scale eddying motion in the respective layers.

We attempted to obtain a measure of this flushing in the embayment by performing some simple tests. The embayment was sealed off from the main basin by inserting a vertical barrier at the throat, dye was injected into the thin lower layer and carefully and uniformly mixed throughout the sealed off lower layer. The flushing experiment was initiated by rocking the tank to create waves, removing the barrier separating the embayment from the main basin, and measuring the dye concentration in the embayment by periodically extracting samples and measuring concentrations in a fluorometer.

After several attempts, only two runs yielded reliable information and, as shown in Figure 7, the results show a rapid decrease of the initial dye concentration for both runs. Since neither run exhibited a simple exponential decay of dye concentration with time, it was not feasible to extract an e -folding timescale as the measure of the flushing time in the usual way. We therefore defined the flushing time as simply the time for the concentration to reduce to 5% of the initial value, yielding flushing times of 5 and 8 rotation periods, respectively, for the two runs in Figure 7.

Maxworthy (1977) showed that when flow was forced from a channel, the circulation in the eddies created by the ejection was closely given by the initial circulation

$$C = \frac{1}{2} \int_0^L V dl \sim \frac{1}{2} V_{av} L \quad (2)$$

where V is the velocity across the width of the embayment entrance, V_{av} the average velocity over the width, and L the length of travel within the embayment.

The vertically integrated layer velocities associated with the Kelvin wave described by equation (1) are given by

$$V_i = \frac{c_i^2}{h_i} \quad i=1, 2. \quad (3)$$

Assuming the velocity varies sinusoidally over the width of the throat

$$C \sim \frac{1}{2} V_{av} \left(V_{av} \frac{T}{2} \right) \sim \frac{1}{2} \left(\frac{c}{\pi} \right)^2 \left(\frac{ca}{h_1} \right)^2 \frac{T}{2} \sim 0.1 \left(\frac{ca}{h_1} \right)^2 T \quad (4)$$

where T is the forcing period. For the experiment shown in Figure 6, $a = 1.5$ cm, $c = 9.2$ cm s^{-1} , $h_1 = 4$ cm and $T = 47$ secs, then from (4) $C \sim 56$ $\text{cm}^2 \text{s}^{-1}$.

For a steady, fully developed turbulent field, the eddy diffusivity $K \sim C$, hence the timescale to flush the embayment of length L would be

$$T_f \sim \frac{L^2}{K} \sim \frac{L^2}{0.1 \left(\frac{ca}{h_1} \right)^2 T} \quad (5)$$

Applying the estimate in (5) to the experiments in Figure 7a with $L = 70$ cm and wave amplitude $a = 1.7$ cm, yields $T_f \sim 3.3$ rotation periods, whereas for the example in Figure 7b with wave amplitude $a = 1.5$ cm yields $T_f \sim 7.1$ rotation periods, consistent with the results shown in Figure 7.

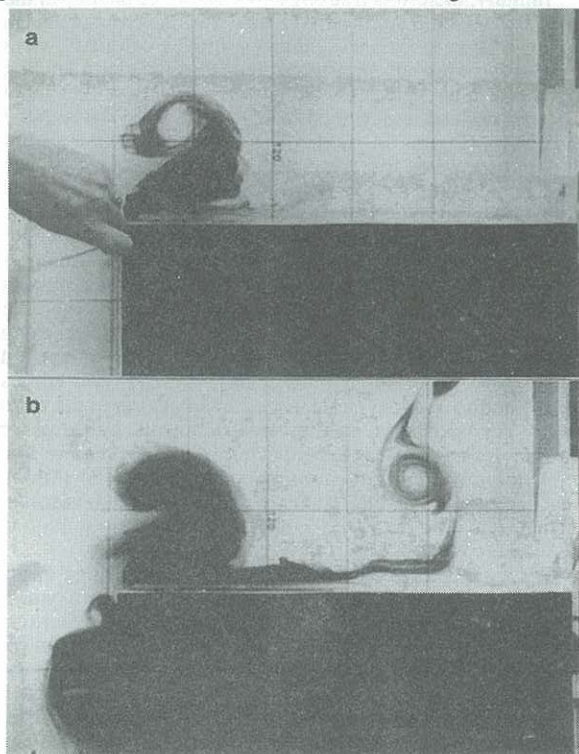


Figure 6. Dye injection study of an experiment running at steady state with a forcing period of 47 seconds. Parameters are $h_1 = 4.0$ cm, $h_2 = 14.3$ cm, $g' = 27.1$ cm s^{-2} and $f = 0.86$ rs^{-1} . The time between photographs, in rotation periods, are a) 0.00 b) 1.3

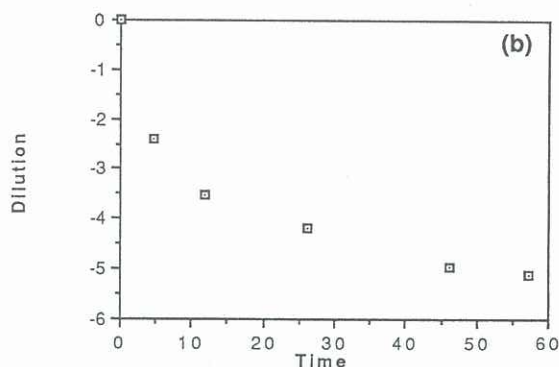
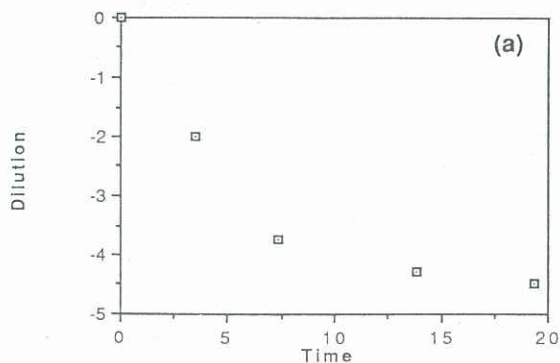


Figure 7. Dilution as a function of time in, rotation periods, for the two embayment flushing studies. Dilution is defined as $\ln(C/C_0)$ where C is the concentration and C_0 the initial concentration. Parameters are a) $h_1 = 4.0$ cm, $h_2 = 14.3$ cm, $g' = 27.2$ cm s^{-2} and $f = 0.58$ rs^{-1} . b) $h_1 = 4.0$ cm, $h_2 = 16.0$ cm, $g' = 27.2$ cm s^{-2} and $f = 1$ rs^{-1} .

CONCLUSIONS

The observations described above demonstrate that when forced by tilting of the tank, the resulting internal wave is dominated by the cyclonic propagation of Kelvin waves around the tank. When forced in a steady harmonic manner, the amplitude of the Kelvin wave is maximised when the forcing frequency corresponds to the natural frequency of the basin, defined by the speed of propagation of the Kelvin wave and the length of the basin perimeter. Dye injection studies indicate that as the Kelvin waves enter the embayment, considerable stirring occurs when the Burger number is of order one. Eddies are created as the flow separates from the sharp leading edge of the embayment. As a consequence, the embayment is flushed, not so much by vertical mixing associated with the small scale shear across the interface in the embayment, but predominantly due to the horizontal large scale eddy stirring in each of the two layers.

REFERENCES

- Csanady, G.T. and Scott J. L. (1974) Baroclinic coastal jets in Lake Ontario during IFYGL. *J.Phys. Oceanogr.*, 4: 524-541.
- Hamblin, P.F. (1978) Internal Kelvin waves in a fjord lake. *J. Geophys. Res.*, 83:287-300.
- Ivey, G.N. (1987) Boundary mixing in a rotating stratified fluid. *J. Fluid Mech.*, 121:1-26.
- Maxworthy, T. (1977) Some experimental studies of vortex rings. *J. Fluid Mech.*, 81:465-495.
- Mortimer, C.H. (1963) Frontiers in physical limnology with particular reference to long waves in rotating basins. *Proc. 5 th Conf. Great Lakes Res.*, Univ. of Michigan, Great Lakes Div., Rep. No. 9.
- Mortimer, C.H. (1974) Lake Hydrodynamics. *Mitt. Int. Ver. Theor. Angew. Limnol.*, 20: 124-197.
- Okamoto, I. (1991) Water mass exchange between the North Basin and Shioza, in *Physics in Lake Biwa*, J. Imberger (ed.).
- Renouard, D.P. (1981) An experimental study of gravity-inertial waves and wind-induced Kelvin-type upwellings in a rotating system. *J.Phys. Oceanogr.*, 11: 1100-1112.
- Zenger, O. (1989) Ursachen und auswirkungen von transport- und mischungs- prozessen im Westlichen Bodensee. PhD dissertation, Ruprecht-Karls-Universitat, Heidelberg (in German).

We would like to thank K. Zic and C. Patriatchi for comments on this paper. This work is supported by the Australian Research Council. Environmental Dynamics Report ED-722-GI.